Studies on the Removal of Phosphate from Drinking Water by Electrocoagulation Process

Subramanyan Vasudevan,* Ganapathy Sozhan, Subbiah Ravichandran, Jeganathan Jayaraj, Jothinathan Lakshmi, and Sagayaraj Margrat Sheela[†]

Central Electrochemical Research Institute (CSIR), Karaikudi 630 006, India

The present study provides an electrocoagulation process for the removal of phosphate from drinking water using mild steel as the anode and stainless steel as the cathode. The studies were carried out as a function of pH, temperature, current density, and so forth, and the adsorption capacity was evaluated using both Langmuir and Freundlich isotherm models. The results showed that the maximum removal efficiency of 98% was achieved at a current density of 0.05 A·dm^{-2} at a pH of 6.5. The adsorption of phosphate preferably fitting the Langmuir adsorption isotherm suggests monolayer coverage of adsorbed molecules. The adsorption process follows second-order kinetics. Temperature studies showed that adsorption was endothermic and spontaneous in nature.

Introduction

As is well known, eutrophication is one of the main problems nowadays encountered in the monitoring of environmental water sources in industrialized countries. This phenomenon, which is responsible for the dramatic growth of algae occurring in drinking water, is caused by the excess phosphate concentration in the effluents from municipal or industrial plants discharged to the environment. In the countryside, where agriculture and animal husbandry are the main industries, wastes from these activities will contribute to the accumulation of phosphorus in soil and water bodies. These phosphorus compounds, dissolved in surface or groundwaters, are responsible for eutrophication in closed water systems, especially in lakes and enclosed bays where the water is almost stagnant.[1] The U.S. discharge limit of phosphate is 0.5–1.0 mg·P/L. The Indian discharge limits for phosphate is 5 mg·P/L[2].

To meet water quality standards, further treatment of water is required. Phosphate removal from wastewater has received considerable attention since the late 1960s.[3] Phosphate removal techniques fall into three main categories: physical, chemical, and biological. Physical methods have proven to be either too expensive, as in the case of electrodialysis and reverse osmosis, or inefficient, removing only 10% of the total phosphate.[4] Chemical treatment is widely used for phosphate removal. The common chemicals used for treatments are aluminum sulfate and ferric chloride. At present, chemical treatments are not used due to disadvantages like high costs of maintenance, problems of sludge handling and its disposal, and neutralization of the effluent.[5–7] In a biological treatment plant, it is necessary to transfer phosphate from the liquid to the sludge phase, and the removal efficiency usually does not exceed 30%, which means that remaining phosphate should be removed by another technique.[8] The phosphate removal from wastewater by adsorption using different materials has also been explored. The major disadvantages of this studied adsorbent is low efficiency and high cost.[9–15]

Recent research has demonstrated that electrochemistry offers an attractive alternative to above-mentioned traditional methods for treating wastewaters.[16–22] Electrochemical coagulation, which is one of these techniques, is the electrochemical production of destabilization agents that brings about charge neutralization for pollutant removal, and it has been used for water or wastewater treatment. Usually, aluminum or iron plates are used as electrodes in the electrocoagulation process. Electrochemically generated metallic ions from these electrodes can undergo hydrolysis near the anode to produce a series of activated intermediates that are able to destabilize the finely dispersed particles present in the water/wastewater to be treated. The destabilized particles then aggregate to form flocs.[23]

(i) When aluminum is used as electrode, the reactions are as follows:

At the cathode,

$$2H_2O + 2e^- \rightarrow H_2(g) + 2OH^- \tag{1}$$

At the anode,

$$Al \rightarrow Al^{3+} + 3e^- \tag{2}$$

In the solution,

$$Al^{3+}(aq) + 3H_2O \rightarrow Al(OH)_3 + 3H^+(aq) \tag{3}$$
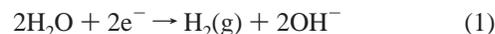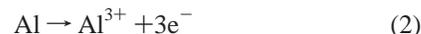
(ii) When iron is used as electrode, the reactions are as follows:

At the cathode,

$$2H_2O + 2e^- \rightarrow H_2(g) + 2OH^- \tag{4}$$

At the anode,

$$4Fe(s) \rightarrow 4Fe^{2+}(aq) + 8e^- \tag{5}$$
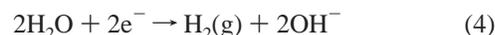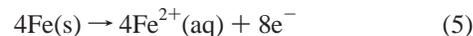
and with dissolved oxygen in solution,

$$4Fe^{2+}(aq) + 10H_2O(l) + O_2(g) \rightarrow 4Fe(OH)_3 + 8H^+(aq) \tag{6}$$

overall reaction,

$$4Fe(s) + 10H_2O(l) + O_2(g) \rightarrow Fe(OH)_3(s) + 4H_2(g) \tag{7}$$
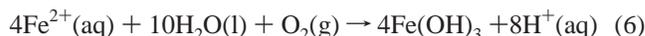
The advantages of electrocoagulation include high particulate removal efficiency, a compact treatment facility, relatively low cost, and the possibility of complete automation.[24–25] This

---

  * To whom correspondence should be addressed. Tel.: 91 4565 227554. Fax: 91 4565 227779. E-mail: vasudevan65@gmail.com.
  [†] St. Joseph College.
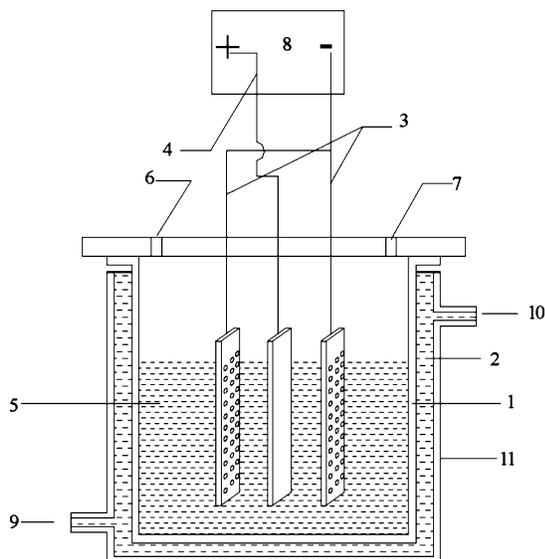
Figure 1. Laboratory scale cell assembly, (1) cell; (2) thermostatic water; (3) stainless steel cathode; (4) anode; (5) electrolyte; (6) and (7) holes to introduce pH sensor and thermometer; (8) dc source; (9) inlet of thermostatic water; (10) outlet of thermostatic water; and (11) thermostat.

Figure 2. Effect of agitation time and initial phosphate concentration on the amount of phosphate adsorbed. Conditions, electrolyte pH 6.5; electrolyte temperature, 305 K; current density, 0.05 A·dm^{-2}.

method is characterized by reduced sludge production, a minimum requirement of chemicals, and ease of operation.[26] Although there are numerous reports related with electrochemical coagulation as a means of removal of many pollutants from water and wastewater, there is limited work on phosphate removal by the electrochemical method and its adsorption and kinetics studies. This article presents the results of the laboratory scale studies on the removal of phosphate using mild steel and stainless steel as the anode and cathode respectively by the electrocoagulation process. In doing so, the equilibrium adsorption behavior is analyzed by fitting models of Langmuir and Freundlich isotherms. Adsorption kinetics of electrocoagulants is analyzed using first- and second-order kinetic models. Activation energy is evaluated to study the nature of adsorption.

Materials and Methods

Cell Construction and Electrolysis. The electrolytic cell (Figure 1) consisted of a 1.0 L Plexiglas vessel that was fitted with a poly(vinyl chloride) cell cover with slots to introduce the electrodes, pH sensor, a thermometer, and the electrolytes. Mild steel (Commercial Grade, India) with a surface area of 0.02 m^2 acted as the anode. The cathode was a stainless steel (SS 304; SAIL, India) sheet of the same size as the anode and placed at an interelectrode distance of 0.005 m. The temperature of the electrolyte was controlled to the desired value with a variation of ±2 K by adjusting the rate of flow of thermostatically controlled water through an external glass-cooling spiral. A regulated direct current was supplied from a rectifier (10 A, 0−25 V; Aplab model).

The phosphate (KH$_2$PO$_4$) (Analar Reagent) was dissolved in tap (drinking) water for the required concentration. A 0.90 L portion of solution was used for each experiment, which was used as the electrolyte. The pH of the electrolyte was adjusted, if required, with 1 M HCl and 1 M NaOH solutions before adsorption experiments.

Analysis. The analysis of phosphate was carried out using the yellow vanodomolybdophosphoric acid method by a double beam spectrophotometer according to the Standard Methods for Examination of Water and Wastewater.[27]

Electrocoagulatioan byproducts were analyzed by a JEOL X-ray diffractometer (Type − JEOL, Japan). The surface
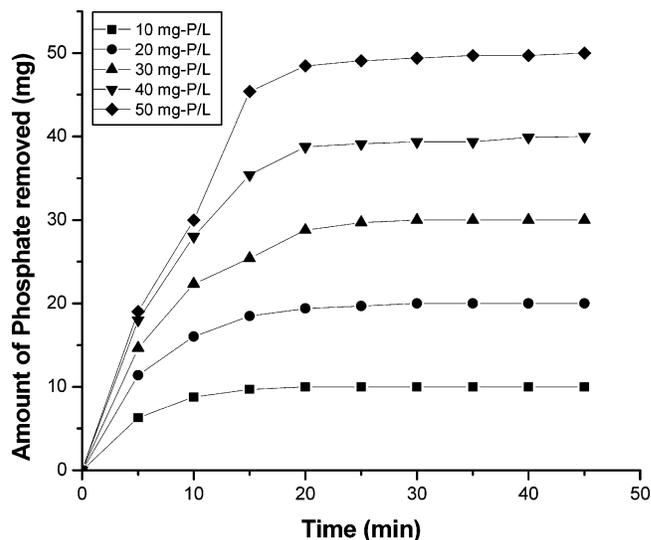
morphology of the anode before and after treatment was analyzed by a metallurgical microscope made by ZEISS, Germany.

Results and Discussion

Effect of Initial Phosphate Concentration. As seen from Figure 2, the adsorption of phosphate is increased with an increase in phosphate concentration and remains constant after the equilibrium time. The equilibrium time was 20 minutes for all of the concentrations studied (10−50 mg·P/L). The amount of phosphate adsorbed (q) increased from 10 to 48.46 mg as the concentration was increased from 10 to 50 mg·P/L. The figure also shows that the adsorption is rapid in the initial stages and gradually decreases with the progress of adsorption. The plots are single, smooth, and continuous curves leading to saturation, suggesting the possible monolayer coverage to phosphate on the surface of the adsorbent.[28]

Effect of Current Density. The amount of phosphate removal and the removal rate have increased by increasing the current density. The removal efficiencies are 68, 72, 88, 92, and 98% for current densities of 0.01, 0.02, 0.03, 0.04, and 0.05 A·dm^{-2}, respectively. The results are presented in Table 1. Further, the amount of phosphate removal depends upon the quantity of adsorbent generated, which is related to the time and current density.[29−31] As expected, the amount of phosphate adsorption increases with the increase in current density, which indicates that the adsorption depends upon the availability of binding sites for phosphate.

Effect of pH. The pH is one of the important factors affecting the performance of the electrochemical process. To examine this effect, a series of experiments were carried out using 100 mg·P/L phosphate-containing solutions, with an initial pH varying in the range of 2−12. The removal efficiency of phosphate was increased with increasing the pH and the maximum removal efficiency as obtained at pH 6.5. It is found that (Figure 3) the maximum removal efficiency for the removal of phosphate is 98% at pH 6.5, and the minimum efficiency is 60% at pH 12. At acidic pHs, the oxide surfaces exhibit a net positive charge, and adsorption of anionic phosphate is enhanced by columbic attraction. At higher pHs, the oxide surface has a net negative charge and would tend to repulse the anionic phosphate in solution. Therefore, the maximum amount of phosphate removal occurred at pH 6.5.
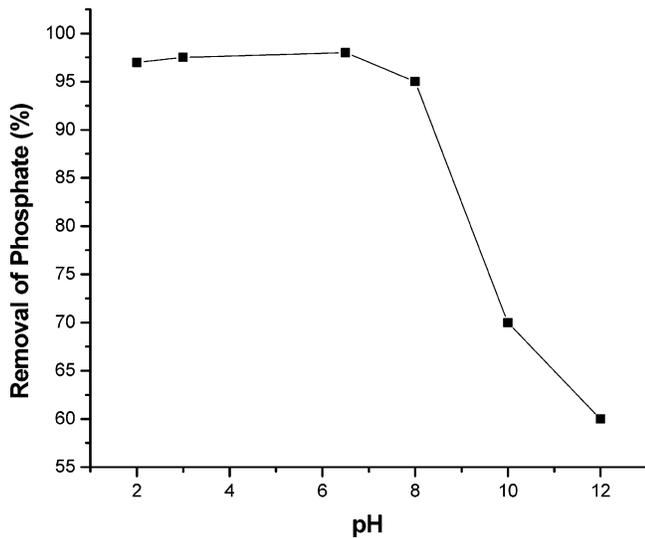
Figure 3. Effect of pH on the removal of phosphate. Conditions, concentration of phosphate, 100 mg·P/L; current density, 0.05 A·dm^{-2}; agitation time, 60 min; electrolyte temperature, 305 K.
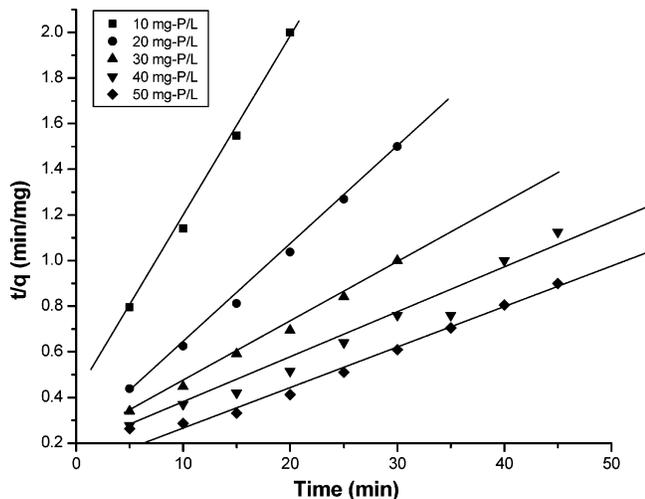
Figure 4. Second-order kinetic model plot of different concentrations of phosphate. Conditions, electrolyte pH 6.5; electrolyte temperature, 305 K; current density, 0.05 A·dm^{-2}.

Adsorption Kinetics. The adsorption kinetic data of phosphate are analyzed using the Lagergran rate equation. The first-order Lagergran model is,[32]

$$dq/dt = k_1(q_e - q) \tag{8}$$

where q is the amount of phosphate adsorbed on the adsorbent at time t (min), and k_1 (min^{-1}) is the rate constant of first-order adsorption. The integrated form of the above equation is,

$$\log(q_e - q) = \log(q_e) - k_1 t/2.303 \tag{9}$$

where q_e is the amount of phosphate adsorbed at equilibrium. The q_e and rate constant (k_1) were calculated from the slope of the plots of $\log(q_e - q)$ versus time (t). A straight line obtained from the plots suggests the applicability of this kinetic model. It was found that the calculated q_e values do not agree with the experimental values (figure not shown here). So, the adsorption does not obey the first-order kinetics adsorption.

The second-order kinetic model is expressed as,[33]

$$dq/dt = k_2(q_e - q)^2 \tag{10}$$

Table 1. Effect of Current Density for the Removal of Phosphate from Drinking Water[a]

			Concentration of PO$_4$−P (mg/L)			
Sl. no.	current density (A·dm^{-2})	voltage (V)	initial	final	removal efficiency (%)	final pH
1	0.01	1.0	100	32	68	7.1
2	0.02	1.1	100	28	72	7.1
3	0.03	1.3	100	12	88	7.2
4	0.04	1.3	100	8.0	92	7.2
5	0.05	1.5	100	2.0	98	7.3

[a] Conditions. pH of the electrolyte, 6.5; temperature, 305 K; anode, mild steel; cathode, stainless steel.

Table 2. Comparison Between the Experimental and Calculated q_e Values for Different Initial Phosphate Concentrations in Second Order Adsorption Isotherm at Temperature 305 K and pH 6.5

initial concentration of phosphate (mg·P/L)	q_e experimental (mg)	k_2 (min/mg)	q_e calculated (mg)	R^2
10	10.000	0.015	9.90	0.9965
20	19.386	0.006	19.18	0.9985
30	28.775	0.003	26.86	0.9987
40	38.770	0.002	37.59	0.9856
50	48.465	0.012	48.53	0.9899

where k_2 is the rate constant of the second-order adsorption. The integrated form of eq 10 is

$$1/(q_e - q) = 1/q_e + k_2 t \tag{11}$$

Equation 11 can be rearranged and linearized as,

$$t/q = 1/k_2 q_e^2 + t/q_e \tag{12}$$

The plot t/q versus time (t) (Figure 4) shows a straight line. The second-order kinetic values of q_e and k_2 were calculated from the slope and intercept of the plots t/q versus t (Figure 4). The plot shows that the correlation coefficient for the second-order kinetic model obtained in all of the concentrations studies were above 0.99, and also the calculated q_e values agree with the experimental q_e values. Table 2 depicts the computed result obtained from the second-order kinetic model. These results indicate that the adsorption system studied belongs to the second-order kinetic model. Similar phenomena have been observed in the adsorption of phosphate in Fe(III)/Cr(III) hydroxide.[28]

Adsorption Isotherm. The adsorption capacity of the adsorbent has been tested using Freundlich[31] and Langmuir[28] isotherms. To determine the isotherms, the initial pH was kept at 6.5 and the concentration of phosphate used was in the range of 10−50 mg·P/L. The general form of Freundlich adsorption isotherm is represented by[34]

$$q_e = KC^n \tag{13}$$

Equation 13 can be linearized in logarithmic form, and the Freundlich constants can be determined as follows[35]

$$\log q_e = \log k_f + n \log C_e \tag{14}$$

where k_f is the Freundlich constant related to adsorption capacity, n is the energy or intensity of adsorption, and C_e is the equilibrium concentration of the phosphate (mg/L). To determine the isotherms, the phosphate concentration used was 10−50 mg·P/L at initial pH 6.5. The Freundlich constants k_f and n values are 0.5 and 0.88, respectively. From the analysis of the results,
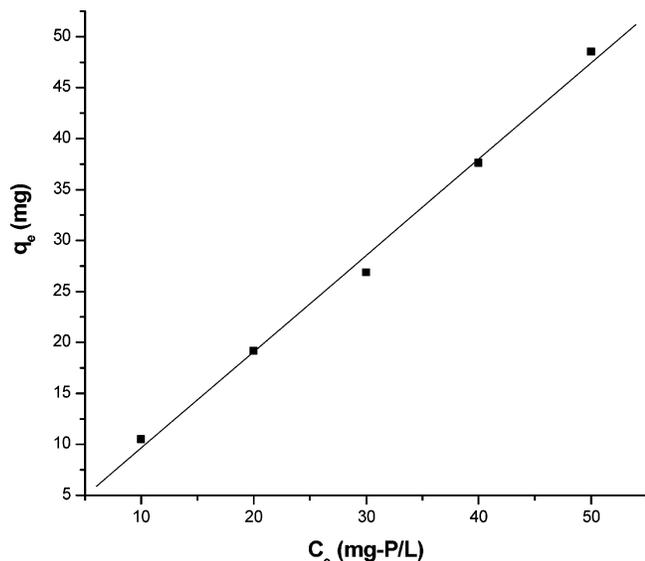
Figure 5. Langmuir plot (q_e vs C_e). Conditions, electrolyte pH 6.5; electrolyte temperature, 305 K; current density, 0.05 A·dm^{-2}.
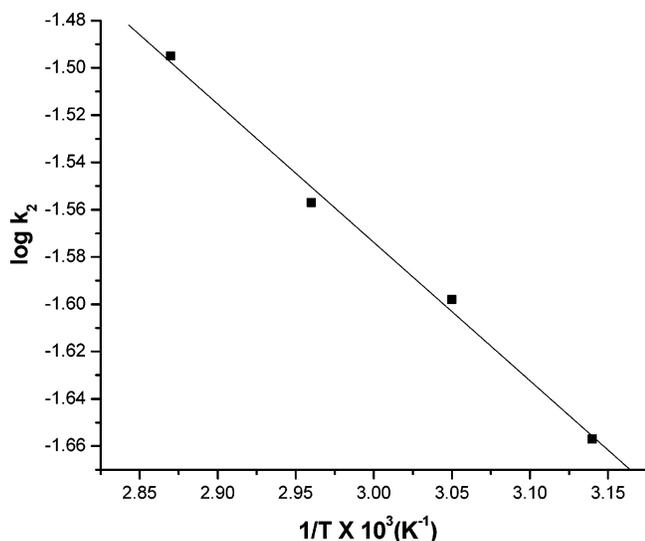
Figure 7. Plot of ln K_c and $1/T$. Conditions, electrolyte pH 6.5; concentration of phosphate, 20 mg·P/L; current density, 0.05 A·dm^{-2}.

Figure 6. Plot of log k_2 and $1/T$. Conditions, electrolyte pH 6.5; concentration of phosphate, 20 mg·P/L; current density, 0.05 A·dm^{-2}.

Figure 8. XRD diffractogram of electrocoagulation byproduct.

Table 3. Langmuir Constants for the Adsorption of Phosphate at Temperature 305 K and pH 6.5

concentration of phosphate (mg·P/L)	q_0 (mg)	b (L)	R_L
10	5.00	0.83	0.107
20			0.056
30			0.038
40			0.029
50			0.023

Table 4. Pore Diffusion Coefficients for the Adsorption of Phosphate at Temperature 305 K and pH 6.5

initial PO_4^{3-} concentration (mg·P/L)	pore diffusion constant $D \times 10^{12}$ (cm^2/s)
10	1.258
20	1.140
30	0.9
40	0.90
50	1.2

it is found that the Freundlich plots do not fit satisfactorily with the experimental data obtained in the present study (figure not shown). This agrees well with the results presented in the literature.[28]

Hence, the Langmuir isotherm has been used to study the surface monolayer adsorption with uniform energies of adsorption on the surface and no transmigration of adsorbate in the plane of the surface. The Langmuir isotherm is expressed as,[36]

$$C_e/q_e = 1/q_o b + C_e/q_o \qquad (15)$$

where C_e is the concentration of the phosphate solution (mg/L) at equilibrium, q_o is the adsorption capacity (Langmuir constant), and b is the energy of adsorption. Figure 5 shows the Langmuir plot with experimental data. The Langmuir plot is a better fit with the experimental data compare to Freundlich plots. The value of the adsorption capacity q_o was found to be 5 mg, which is higher than that of other adsorbents studied.[28] The lower value of the adsorption capacity of the adsorbent studied is due to the pH of the solution, which was found to be >8.0. This condition is not favorable for the adsorption of phosphate (Figure 8).

The essential characteristics of the Langmuir isotherm can be expressed as the dimensionless constant R_L,[37]

$$R_L = 1/(1 + bc_o) \qquad (16)$$

Table 5. Pore Diffusion Coefficients for the Adsorption of Phosphate at pH 6.5 and 20 mg·P/L

temperature (K)	pore diffusion constant $D \times 10^{12}$ (cm²/s)
313	1.14
323	1.63
333	1.66
343	1.75
353	1.84

Table 6. Thermodynamic Parameters for the Adsorption of Phosphate

temperature (K)	K_c	$\Delta G°$ (kJ/mol)	$\Delta H°$ (kJ/mol)	$\Delta S°$ (J/mol K)
313	3.03	−8.013	20.94	91.77
323	3.22	−8.782		
333	3.45	−9.701		
343	4.16	−12.040		

Table 7. Comparison Between the Experimental and Calculated q_e Values for Initial Phosphate Concentration 20 mg·P/L in a Second-Order Adsorption Isotherm at Various Temperatures (pH 6.5)

temperature (K)	q_e experimental (mg)	k_2 min/mg	q_e calculated (mg)	R^2
303	19.386	0.006	19.18	0.9985
313	19.079	0.022	19.20	0.9991
323	19.079	0.025	19.19	0.9993
333	19.386	0.027	19.58	0.9994
343	19.693	0.032	20.00	0.9996

where R_L is the equilibrium constant, which indicates the type of adsorption b, and c_o is the Langmuir constant. The R_L values between 0 and 1 indicate a favorable adsorption. The R_L values were found to be between 0 and 1 for all of the concentrations of phosphate studied. The results are presented in Table 3.

Effect of Temperature. The amount of phosphate adsorbed on the adsorbent increases by increasing the temperature, indicating the process to be endothermic.[38] The diffusion coefficient (D) for the intraparticle transport of a PO_4^{3-} species into the adsorbent particles has been calculated at different temperature by,

$$t_{1/2} = 0.03(r_o^2/D) \qquad (17)$$

where $t_{1/2}$ is the time of half adsorption (s), r_o is the radius of the adsorbent particle (cm), and D is the diffusion coefficient in cm²/s. If pore diffusion is to be the rate-limiting step, D should be the range 10^{-11} to 10^{-13} cm²/s for various temperatures in all of the concentrations.[28] In the present work, D is found to be in the range of 10^{-12} cm²/s, which shows that the pore diffusion of PO_4^{3-} is the rate-limiting step. The pore diffusion coefficient (D) values for different initial concentrations of PO_4^{3-} and temperature are presented in Table 4 and Table 5, respectively.

To find out the energy of activation for the adsorption of phosphate, the second-order rate constant is expressed in the Arrhenius form,[29]

$$\ln k_2 = \ln k_o - E/RT \qquad (18)$$

where k_o is the constant of the equation (g/mg·min⁻¹), E is the energy of activation (J/mol), R is the gas constant (8.314 J/mol K), and T is the temperature in K. Figure 6 shows that the rate constants vary with temperature according to eq 18. The activation energy (11.03 kJ/mol) is calculated from slope of the fitted equation. The K_c and ΔG values are calculated and
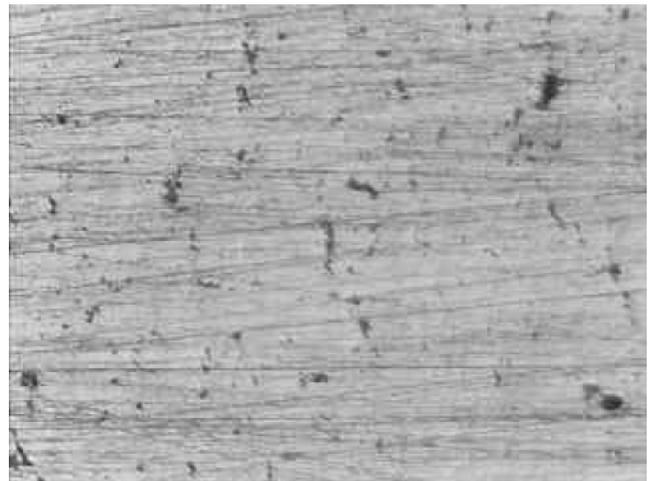
(a)
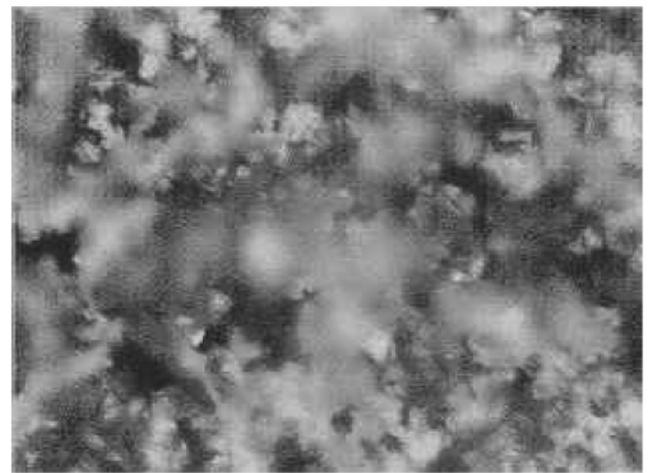
(b)

Figure 9. Microscopic image of the anode (a) before and (b) after treatment.

presented in Table 6. From the table, it is found that the negative value of ΔG indicates a spontaneous nature of adsorption.

Other thermodynamic parameters such as entropy change (ΔS) and enthalpy change (ΔH) were determined using the van't Hoff equation

$$\ln K_c = \frac{\Delta S}{R} - \frac{\Delta H}{RT} \qquad (19)$$

The enthalpy change (ΔH) and entropy change (ΔS) were obtained from the slope and intercept of the van't Hoff linear plots of $\ln K_c$ versus $1/T$ (Figure 7). A positive value of enthalpy change (ΔH) indicates that the adsorption process is endothermic in nature, and the negative value of change in internal energy (ΔG) shows the spontaneous adsorption of phosphate on the adsorbent. Positive values of entropy change show the increased randomness of the solution interface during the adsorption of phosphate on the adsorbent (Table 6). Enhancement of the adsorption capacity of the electrocoagulant (Fe(III) hydroxide) at higher temperatures may be attributed to the enlargement of the pore size and or activation of the adsorbent surface. Using the Lagergran rate equation, first-order rate constants and correlation coefficients were calculated for different temperatures (303−343 K). The calculated q_e values obtained from the first-order kinetics do not agree with the experimental q_e values. The second-order kinetics model shows that the calculated q_e values agree with the experimental values (Table 7). This indicates

that the adsorption follows the second-order kinetic model at different temperatures used in this study. From the table, it is found that the rate constant k_2 increased with increasing the temperature from 303 to 343 K. The increase in adsorption may be due to a change in pore size upon increasing in kinetic energy of the phosphate species and the enhanced rate of intraparticle diffusion of the adsorbate.

The electrocoagulation byproduct showed well the crystalline phase such as iron phosphate hydrate, magnetite, iron hydrogen phosphate (Figure 8). Figure 9 shows the microscopic image of the anode before and after treatment. The microscopic image indicates the presence of ultrafine particles of micron size on the surface.

Conclusion

The results showed that the maximum removal efficiency of 98% was achieved at a current density of 0.05A·dm^{-2} and a pH of 6.5 using mild steel as the anode and stainless steel as the cathode. The results indicate that the process can be scaled up to higher capacity and used to eradicate a eutrophication problem. The adsorption of phosphate preferably fitting the Langmuir adsorption isotherm suggests monolayer coverage of adsorbed molecules. The adsorption process follows second-order kinetics. Temperature studies showed that adsorption was endothermic and spontaneous in nature.

Acknowledgment

Literature Cited

(1) Oguzi, E.; Gurses, A.; Yalcin, M. Removal of Phosphate from Wastewaters by Adsorption. *Water, Air, Soil Pollut.* **2003**, *148*, 279−287.

(2) Central Pollution Control Board, Ministry of Environment and Forests, http://www.cpcb.nic.in, Government of of India, Delhi.

(3) Groterud, O.; Smoczynski, L. Phosphorus Removal from Water by Means of Electrolysis. *Water Res.* **1986**, *20*, 667−669.

(4) Yeoman, S.; Stephenson, T.; Lester, J. N.; Perry, R. The Removal of Phosphorus during Wastewater Treatment: A Review. *Environ. Pollut.* **1998**, *49*, 183−233.

(5) Boisvert, J. P.; To, T. C.; Berrak, A.; Jolicoeur, C. Phosphate Adsorption in Flocculation Processes of Aluminium Sulphate and Poly-aluminium-Silicate-Sulphate. *Water Res.* **1997**, *31*, 1939−1946.

(6) Fytianos, K.; Voudrias, E.; Raikos, N. Modelling of Phosphorus Removal from Aqueous and Wastewater Samples Using Ferric Iron. *Environ. Pollut.* **1998**, *101*, 123−130.

(7) Neufeld, R. D.; Thodos, G. Removal of Orthophosphates from Aqueous Solutions with Activated Alumina. *Environ. Sci. Technol.* **1969**, *3*, 661−667.

(8) Stensel, H. D. *Principles of biological phosphorus removal: Phosphorus and Nitrogen Removal from Municipal Wastewater—Principles and Practice*, 2nd ed.; H. K. Lewis: London, 1991.

(9) Li, Y. Z.; Liu, C. J.; Luan, Z. K.; Peng, X. J.; Zhu, C. L.; Chen, Z. Y.; Zhang, Z. J.; Fan, J. H.; Jia, Z. P. Phosphate Removal from Aqueous Solutions Using Raw and Activated Red Mud and Fly Ash. *J. Hazard. Mater.* **2006**, *137B*, 374−383.

(10) Johansson, L.; Gustafsson, J. P. Phosphate Removal Using Blast Furnace Slags and Opoka-Mechanisms. *Water Res.* **2000**, *34*, 259−265.

(11) Kostura, B.; Kulveitová, H.; Leško, J. Blast Furnace Slags as Sorbents of Phosphate from Water Solutions. *Water Res.* **2005**, *39*, 1795−1802.

(12) Oguz, E. Removal of Phosphate from Aqueous Solution with Blast Furnace Slag. *J. Hazard. Mater.* **2004**, *114B*, 131−137.

(13) Karaca, S.; Gürses, A.; Ejer, M.; Açıkyıldız, M. Adsorption Removal of Phosphate from Aqueous Solutions Using Raw and Calcinated Dolomite. *J. Hazard. Mater.* **2006**, *128B*, 273−279.

(14) Yang, Y.; Tomlinson, D.; Kennedy, S.; Zhao, Y. Q. Dewartered Alum Sludge: A Potential Adsorbent for Phosphorus Removal. *Water Sci. Technol.* **2006**, *54*, 207−213.

(15) Lee, S. H.; Lee, B. C.; Lee, W. K.; Lee, S. H.; Choi, Y. S.; Park, K. Y.; Iwamono, M. Phosphorus Recovery by Mesoporous Structure Material from Wastewater. *Water Sci. Technol.* **2007**, *55*, 169−176.

(16) Miwa, D. W.; Malpass, G. R. P.; Machado, S. A. S.; Motheo, A. J. Electrochemical Degradation of Carbaryl on Oxide Electrodes. *Water Res.* **2006**, *40*, 3281−3289.

(17) Onder, E.; Koparal, A. S.; Ogutveren, U. B. An Alternative Method for the Removal of Surfactants from Water: Electrochemical Coagulation. *Sep. Purif. Technol.* **2007**, *52*, 527−532.

(18) Ikematsu, M.; Kaneda, K.; Iseki, M.; Yasuda, M. Electrochemical Treatment of Human Urine for Its Storage and Reuse as Flush Water. *Sci. Total Environ.* **2007**, *382*, 159−164.

(19) Carlesi Jara, C.; Fino, D.; Specchia, V.; Saracco, G.; Spinelli, P. Electrochemical Removal of Antibiotics from Wastewaters. *Appl. Catal., B* **2007**, *70*, 479−487.

(20) Christensen, P. A.; Egerton, T. A.; Lin, W. F.; Meynet, P.; Shaoa, Z. G.; Wright, N. G. A Novel Electrochemical Device for the Disinfection of Fluids by OH Radicals. *Chem. Commun.* **2006**, *38*, 4022−4023.

(21) Carlos A.; Huitle, M.; Ferro, S. Electrochemical Oxidation of Organic Pollutants for the Wastewater Treatment: Direct and Indirect Processes. *Chem. Soc. Rev.* **2006**, *35*, 1324−1340.

(22) Gabrielli, C.; Maurin, G.; Francy-Chausson, H.; Thery, P.; Tran, T. T. M.; Tlili, M. Electrochemical Water Softening: Principle and Application. *Desalination* **2006**, *201*, 150−163.

(23) Chen, X.; Chen, G.; Yue, P. L. Investigation on the Electrolysis Voltage of Electrocoagulation. *Chem. Eng. Sci.* **2002**, *57*, 2449−2455.

(24) Chen, G. Electrochemical Technologies in Wastewater Treatment. *Sep. Purif. Technol.* **2004**, *38*, 11−41.

(25) Adhoum, N.; Monser, L. Decolourization and Removal of Phenolic Compounds from Olive Mill Wastewater by Electrocoagulation. *Chem. Eng. Process.* **2004**, *43*, 1281−1287.

(26) Rajeshwar, K.; Ibanez, J. K. *Environmental Electrochemistry: Fundamentals and Applications in Pollution Abatement*; Academic Press: San Diego, 1997.

(27) APHA, *Standard Methods for Examination of Water and Wastewater;* American Public Health Association: Washington D.C., 1998.

(28) Namasivayam, C.; Prathap, K. Recycling Fe(III)/Cr(III) Hydroxide, an Industrial Solid Waste for the Removal of Phosphate from Water. *J. Hazard. Mater.* **2005**, *123B*, 127−134.

(29) Golder, A. K.; Samantha, A. N.; Ray, S. Removal of Phosphate from Aqueous Solution Using Calcined Metal Hydroxides Sludge Waste Generated from Electrocoagulation. *Sep. Purif. Technol.* **2006**, *52*, 102−109.

(30) Irdemez, S.; Demircioglu, N.; Yildiz, Y. S.; Bingul, Z. The Effects of Current Density and Phosphate Concentration on Phosphate Removal from Waste Water by Electro Coagulation Using Aluminum and Iron Plate Electrodes. *Sep. Purif. Technol.* **2006**, *52*, 218−223.

(31) Groterud, O.; Smoczynski, L. Phosphorus Removal from Water by Means of Electrolysis. *Water Res.* **1986**, *20*, 667−669.

(32) Bina, G.; Begum Zareena, I.; Garima, R. Equilibrium and Kinetic Studies for the Adsorption of Mn(II) and Co(II) from Aqueous Media Using Agar-Agar as Sorbent. *Res. J. Chem. Environ.* **2007**, *11*, 16−22.

(33) Mckay, G.; Ho, Y. s. The Sorption of Lead(II) on Peat. *Water Res.* **1999**, *33*, 578−584.

(34) Namasivayam, C.; Senthil Kumar, S. Removal of Arsenic(V) from Aqueous Solutions Using Industrial Solid Waste: Adsorption Rates and Equilibrium Studies. *Ind. Eng. Chem. Res.* **1998**, *37*, 4816−4822.

(35) Uber, F. H. Die Adsorption in Losungen. *Z. Phys. Chem.* **1985**, *57*, 387−470.

(36) Langmuir, I. The Adsorption of Gases on Plane Surface of Gases on Plane Surface of Glass, Mica and Platinum. *J. Am. Chem. Soc.* **1918**, *40*, 1361−1365.

(37) Michelson, L. D.; Gideon, P. G.; Pace, E. G.; Kutal, L. H. Removal of Solute Mercury from Waste Water by Complexing Technique, U.S. department industry, Office of Water Research and Technology Bulletin, 1975.

(38) Nayak Preeti, S.; Singh, B. K. Sorption Dynamics of Phenol on Naturally Occurring Low Cost Clay. *Res. J. Chem. Environ.* **2007**, *11*, 23−28.